

Vacancy-plane-mediated exfoliation of sub-monolayer 2D pyrrhotite

Jian-Jhang Lee, ^{a,b} Yi-Hung Chu, ^{b,c} Zhi-Long Yen, ^{a,b} Jeyavelan Muthu, ^a Chu-Chi Ting, ^c Ssu-Yen Huang, ^a Mario Hofmann ^a and Ya-Ping Hsieh ^{*b,c}

^a Department of Physics, National Taiwan University, Taipei, Taiwan.

^b Institute of Atomic and Molecular Sciences, Academia Sinica, Taipei, Taiwan. Email:
yphsieh@gate.sinica.edu.tw

^c Graduate Institute of Opto-Mechatronics, National Chung Cheng University, Chiayi, Taiwan

Corresponding Author

* E-mail: yphsieh@gate.sinica.edu.tw (Y. P. H.)

The models and measuring parameters of various instruments

The structure of electrochemically exfoliated pyrrhotite was confirmed by various characterizations such as Raman spectroscopy (532nm laser), Scanning Electron Microscope (SEM, Hitachi S4800-I), and Energy-dispersive X-ray Spectroscopy (EDS, Phenom ProX).

The structure of bulk pyrrhotite was confirmed by the X-ray powder diffractogram (XRPD, PANalytical X'Pert³ Powder).

The thickness and MFM images of the exfoliated pyrrhotite were measured by Atomic Force Microscope (AFM, Force AFM GENIE E7). The parameters of the MFM images were as follows: the mode of operation: Lift Mode; the type of tip: soft magnetic coating on the tip side; the distance of the tip to the sample: 50nm.

The selected area electron diffraction patterns were obtained by Transmission Electron Microscope (TEM, JEM2100F). The hysteresis curve of the synthesized pyrrhotite 4C was recorded by the Superconducting Quantum Interference Device Magnetometer (SQUID, Quantum De-sign MPMS-3).

Energy-dispersive X-ray spectroscopy

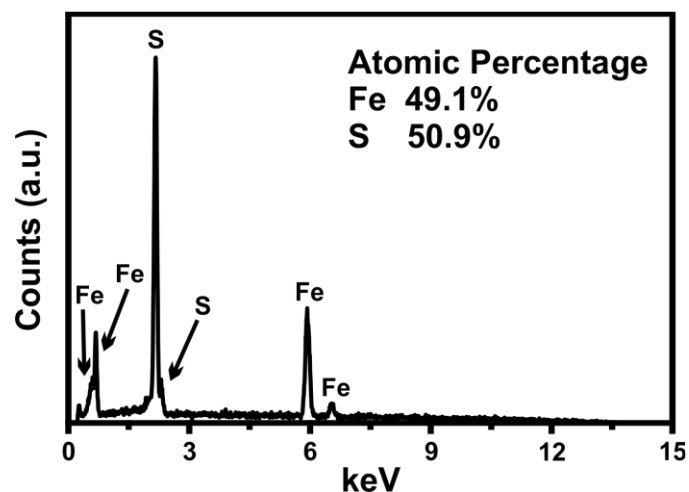


Fig. 1 Elemental analysis from Energy-dispersive X-ray spectroscopy (EDS) reveals a 0.96:1 ratio of Fe and S.

The Raman spectrum comparison with the RRUFF database

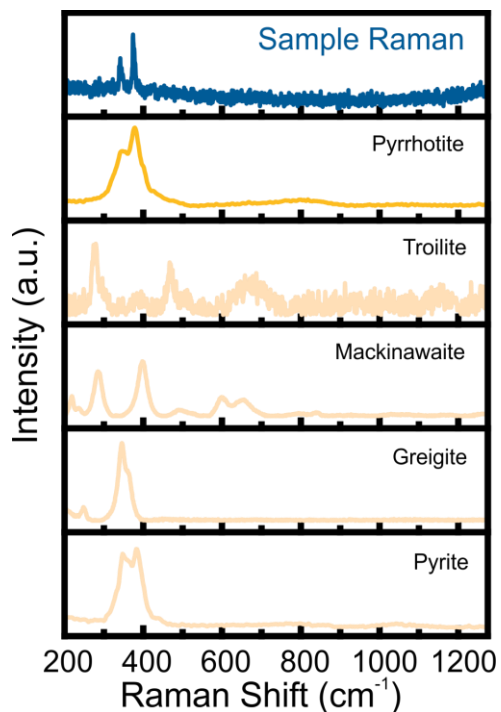


Fig. 2 The Raman characterization for pyrrhotite sample compared with that of various iron sulfide compounds (the contrast data from the RRUFF database: Pyrrhotite Fe_{1-x}S (ID=R060440), Troilite FeS (ID=R070242), Mackinawite Fe_{1+x}S (ID=R060388), Greigite Fe_3S_4 (ID=R120103) and Pyrite FeS_2 (ID=R050070)).

The formation of Cl_2 at a higher overpotential

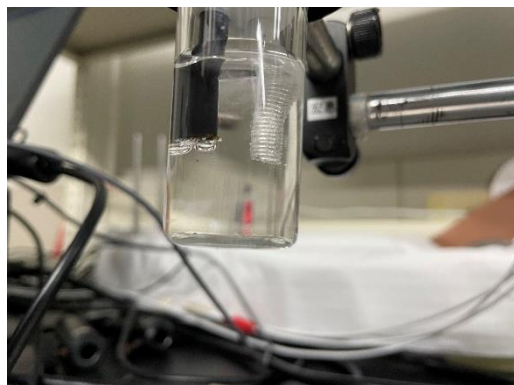


Fig. 3 Upon the formation of Cl_2 at a higher overpotential, the interlayer distance of pyrrhotite is increased, and exfoliation occurs.

The room temperature hysteresis curve per Fe of exfoliated pyrrhotite nanosheets

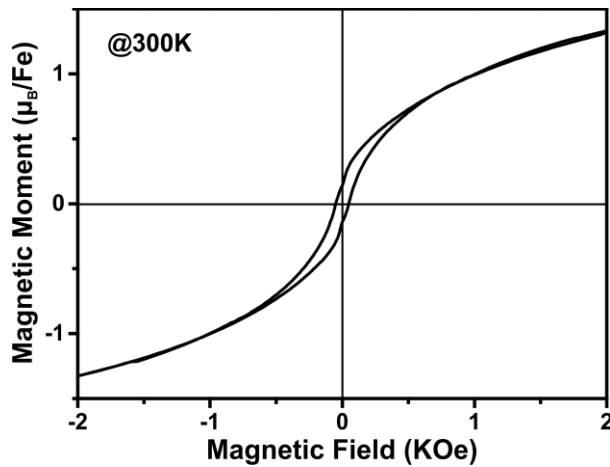


Fig. 4 The room temperature hysteresis figure of exfoliated pyrrhotite nanosheets from SQUID.

The magnetic interaction pathways in hexagonal pyrrhotite structure

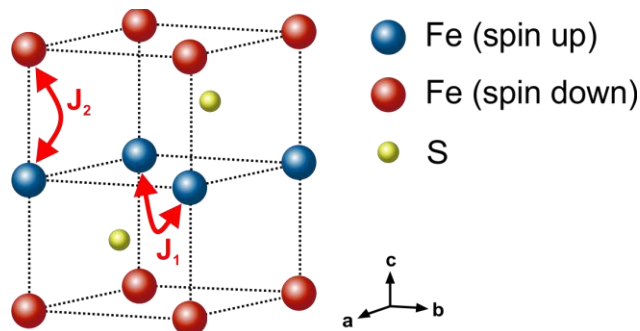


Fig. 5 Schematic representation of the hexagonal NiAs-structure of pyrrhotite with the magnetic interaction pathways.

The temperature-dependence of magnetization of pyrrhotite bulk

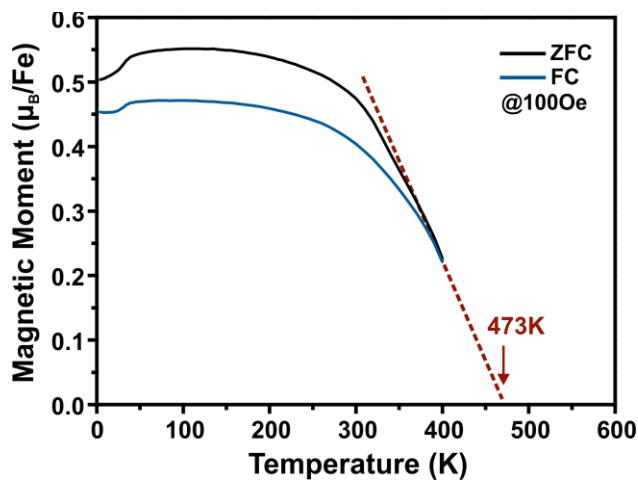


Fig. 6 The magnetization temperature dependence from 400K to 4K. It shows the Curie temperature is about 473K by the graphical method.